Laboratory Investigation (2014) 94, 1260–1272
© 2014 USCAP, Inc All rights reserved 0023-6837/14

MFG-E8 expression for progression of oral squamous cell carcinoma and for self-clearance of apoptotic cells

Manabu Yamazaki[1], Satoshi Maruyama[2], Tatsuya Abé[1,2], Ahmed Essa[1], Hamzah Babkair[1], Jun Cheng[1] and Takashi Saku[1,2]

Milk fat globule—epidermal growth factor (EGF)—factor VIII (MFG-E8) is a secreted glycoprotein that promotes clearance of apoptotic cells by bridging phosphatidylserine on apoptotic cells and integrin $\alpha v\beta 3/5$ on phagocytes. High expression of MFG-E8 has been reported in various types of cancer in humans. Apoptotic figures are frequently found in the surgical samples of oral squamous cell carcinoma (SCC) and carcinoma *in situ*, and we have often observed apoptotic carcinoma cells engulfed by macrophages or even by neighboring carcinoma cells. Thus we hypothesized that MFG-E8 might promote engulfment of apoptotic carcinoma cells by living carcinoma cells and that MFG-E8 expressed by carcinoma cells could contribute to tumor progression. The aim of this study was to elucidate the biological role of MFG-E8 in oral SCC. Fifty-three surgical specimens of oral SCC were used for immunohistochemistry for MFG-E8, and the expression profiles were correlated with clinicopathological properties. Also, we examined the MFG-E8 expression patterns and functions using three human oral SCC cell lines. Most of the cases had MFG-E8-positive SCC cells, and the expression of MFG-E8 was correlated with such clinicopathological features as tumor size, pathological stage, locoregional recurrence, scattering invasion pattern, and SCC cell figures engulfing apoptotic SCC cells. The MFG-E8 staining was enhanced in apoptotic SCC cells, some of which were apparently engulfed by the neighboring SCC cells. ZK-1 cells showed high MFG-E8 expression, and its localization was found in the cytoplasm and the cell surface. Transient MFG-E8 knockdown by siRNA in ZK-1 decreased cell proliferation and invasiveness and increased cell death. Thus we have demonstrated that MFG-E8 promotes tumor progression in oral SCC and that it might be involved in the clearance of apoptotic SCC cells by living SCC cells.

Laboratory Investigation (2014) **94,** 1260–1272; doi:10.1038/labinvest.2014.108; published online 29 September 2014

Milk fat globule—epidermal growth factor (EGF)—factor VIII (MFG-E8), a secreted glycoprotein also termed lactadherin, was identified initially as a marker of human breast cancer[1] and later as a major component of milk fat globule membranes in the murine lactating mammary gland.[2] MFG-E8 is a multifunctional protein that has key roles in apoptotic cell clearance,[3] cellular adhesion between sperm and oocyte,[4] morphogenetic and homeostatic regulation in diverse tissues,[5–7] and angiogenesis.[8] Human MFG-E8 contains two repeats of an EGF-like domain on the N-terminal side and two repeated domains homologous to blood coagulation factor V/VIII on the C-terminal side.[9–11] On the removal of apoptotic cells, MFG-E8 secreted by phagocytes binds to phosphatidylserine on the apoptotic cell surface via the factor V/VIII-like domains, as well as to integrin $\alpha v\beta 3/5$ on the plasma membrane of phagocytes via its RGD sequence within the EGF-like domain.[3] Impaired MFG-E8-mediated uptake of apoptotic cells results in autoimmune diseases in MFG-E8-deficient mice,[12] indicating that it is related to immune tolerance induction.[13]

Apoptotic cells are cleared in MFG-E8-dependent mechanisms, not only by professional phagocytes such as macrophages and dendritic cells but also by non-professional phagocytes, such as epithelial[14] and endothelial cells.[15] During the involution of murine mammary glands, mammary epithelial cells phagocytose apoptotic ones in an MFG-E8-dependent manner.[14] Angiogenic endothelial cells in and around the tumor have MFG-E8-dependent phagocytic properties for apoptotic cells or aged erythrocytes.[15]

In addition to phagocytotic events, the MFG-E8 expressions are also known to be upregulated in neoplastic conditions,

[1]Division of Oral Pathology, Department of Tissue Regeneration and Reconstruction, Niigata University Graduate School of Medical and Dental Sciences, Niigata, Japan and [2]Oral Pathology Section, Department of Surgical Pathology, Niigata University Hospital, Niigata, Japan
Correspondence: Professor T Saku, DDS, PhD, Division of Oral Pathology, Department of Tissue Regeneration and Reconstruction, Niigata University Graduate School of Medical and Dental Sciences. 2-5274 Gakkocho-dori, Chuo-ku, Niigata 951-8514, Japan.
E-mail: tsaku@dent.niigata-u.ac.jp

Received 28 January 2014; revised 9 July 2014; accepted 10 July 2014

including breast cancer,[1,16,17] malignant melanoma,[18,19] bladder tumors,[20] and ovarian cancer.[21] The MFG-E8 expression has been correlated to their progressions[18–20] and to poor clinical outcome.[19] Regarding neoplasms of keratinocytic origin, MFG-E8 has been demonstrated in experimentally induced skin tumors in mice, in which the reduced expression of MFG-E8 was correlated with cellular differentiation.[22] However, MFG-E8 profiles in human keratinocytes or keratinocytic lesions remain entirely unknown.

In our daily practice of diagnostic histopathology, on the other hand, we often encounter apoptotic figures of squamous epithelial cells in oral epithelial lesions, such as lichen planus and squamous cell carcinoma (SCC). In addition, it is not so rare to observe that apoptotic SCC cells have been engulfed by macrophages or even by neighboring SCC cells themselves in surgical samples of oral SCC or carcinoma *in situ*. Thus, based on such clinical experiences and on those lines of evidence mentioned above, we have formulated hypotheses that MFG-E8 expression enhancement is positively related to the progression of oral SCC and that MFG-E8-involved phagocytosis occurs in oral SCC cells. To confirm these hypotheses, we studied MFG-E8 expression patterns in surgical specimens of oral SCC and analyzed primary functions of MFG-E8 in cell proliferation, migration, and invasiveness in oral SCC cells in culture.

MATERIALS AND METHODS

Clinical Samples

This study included 53 consecutive patients who received primary surgical treatment for oral SCC at Niigata University Hospital during a 2-year period from January 2008 to December 2009. The median age of the patients was 67 years (range 22–88 years, mean age 64.7 years), and 24 patients (45.3%) were women. Clinical information was obtained from the patients' medical records. Until December 2012, six patients had local recurrences, and nine had late cervical lymph node metastases. Their surgical specimens containing carcinoma *in situ* foci in addition to the main foci of SCC were fixed in 10% formalin, and the size and gross appearances of the tumors were recorded. The entire specimens were sliced and embedded in paraffin. Serial sections were cut at 4 μm, and one set of sections was stained with hematoxylin and eosin (HE) to confirm their original pathological diagnoses, while the other sets were used for immunohistochemistry. Mirror sectioning techniques[23] were used in some of the cases to demonstrate comparative immunohistochemical profiles between different molecules. Histopathological factors, such as tumor size, tumor depth, pathological T category, lymph node status, pathological disease stage, tumor cell differentiation, and the presence or absence of phagocytic figures of apoptotic SCC cells by neighboring SCC cells, were determined on HE-stained sections. Scattering invasion patterns were assessed by immunohistochemistry for pan-keratin. The experimental protocol for analyzing surgical materials was reviewed and approved by the Ethical Board of Niigata University Graduate School of Medical and Dental Sciences (Oral Life Science).

Cells

Human SCC cell lines (ZK-1, ZK-2, and MK-1) were established from SCCs of the tongue (ZK-1 and ZK-2) and a lymph node focus metastasized from a SCC of the gingiva (MK-1). These cells were maintained in Dulbecco's modified Eagle's medium (DMEM) (Gibco, Life Technologies, Carlsbad, CA, USA) containing 10% fetal calf serum (FCS), 50 μg/ml streptomycin, and 50 IU/ml penicillin (Gibco) under a humidified 5% CO_2/95% air atmosphere at 37 °C. THP-1, a human monocytic leukemia cell line, obtained from Cell Resource Center for Biomedical Research, Institute of Development, Aging and Cancer, Tohoku University, was maintained in RPMI-1640 (Gibco) containing 10% FCS and streptomycin/penicillin.

Antibodies

A mouse monoclonal antibody against MFG-E8 (clone MFG-06, IgG_1), used for immunohistochemical staining, was obtained from Santa Cruz Biotechnology, Inc. (Santa Cruz, CA, USA). Another mouse monoclonal antibody against MFG-E8 (EDM45, IgG_1), used for western blotting, was purchased from Thermo Fisher Scientific (Waltham, MA, USA). A mouse monoclonal antibody against pan-keratin (AE1/AE3, IgG_1) and another against CD68 (PG-M1, IgG_3) were purchased from Dako (Glostrup, Denmark). Mouse monoclonal antibodies against β-actin (mAbcam 8226, IgG_1) and against geminin (EM6, IgG_{2a}) were obtained from Abcam plc. (Cambridge, UK) and from Leica Biosystems Newcastle Ltd. (Newcastle, UK), respectively. Polyclonal antibodies against cleaved caspase-3 were obtained from Cell Signaling Technology (Danvers, MA, USA).

Immunohistochemistry

Deparaffinized and rehydrated sections were immersed in 0.3% hydrogen peroxide in methanol for 30 min at room temperature to block endogenous peroxidase activities. For antigen retrieval of MFG-E8 and cleaved caspase-3 staining, sections were autoclaved in Tris-HCl EDTA buffer (pH 9.0) for 10 min at 121 °C. For pan-keratin and CD68, sections were autoclaved in citrate buffer (pH 6.0). After antigen retrieval, the sections were incubated with 2% normal goat serum (Dako) in phosphate-buffered saline (PBS) for 30 min and then with primary antibodies overnight at 4 °C. After washing with PBS three times, the sections were reacted with Envision plus (Dako) for 30 min at room temperature. Peroxidase reaction products were developed with 3, 3′-diaminobenzidine, and the sections were counterstained with hematoxylin. For control experiments, the primary antibodies were replaced with mouse or rabbit preimmune IgG (Dako).

Evaluation of MFG-E8 Expression Levels

Using a representative section of each case, we evaluated MFG-E8 expression levels by area, based on the number of positive cells, and also according to the intensity of MFG-E8 staining. Area scores of 0, 1, or 2 were given when MFG-E8-positive (+) SCC cells occupied <5%, 5–50%, or >50% of SCC tissue areas, respectively. Staining intensities were rated in comparison with those in vascular endothelial cells around SCC foci. Staining intensity scores of 0, 1, or 2 were given when SCC cells showed no staining, weaker staining than vascular endothelial cells, or stronger staining than them, respectively. Sums of the area scores and intensity scores were defined as MFG-E8 expression scores.

Real-Time Reverse Transcription-PCR (RT-PCR)

Total RNA was isolated from the cells using an ISOGEN system (Nippon Gene Co., Ltd., Tokyo, Japan) and reverse transcribed to cDNA with SuperScript III First-Strand Synthesis System (Life Technologies). Real-time RT-PCR was carried out with specific primers for MFG-E8 using a MiniOpticon Real-Time PCR Detection System CFB-3120 (Bio-Rad Laboratories, Inc., Hercules, CA, USA). Amplification of target genes was monitored in real time, and gene expression levels were quantified using the CFX Manager software version 2.1 (Bio-Rad). The expression of β-actin was used to normalize for variance, and the expression levels of specific genes were represented as ratios to those of β-actin from the same master reaction. PCR primer pairs (5′ to 3′) used for each gene were as follows: MFG-E8, 5′-GTGCGT GTGACCTTCTTG-3′ and 5′-ACCTGTTACCCACATCCT-3′; β-actin, 5′-TCACCCACACTGTGCCCATCTACGA-3′ and 5′-CAGCGGAACCGCTCATTGCCAATGG-3′.

RNA Interference (RNAi)

RNAi experiments were performed using a Stealth RNAi siRNA Duplex Oligoribonucleotides System (Life Technologies). Three different siRNAs for MFG-E8 (#1, 5′-AAACAAGUUC UUCUUGUGGGAGUGG-3′; #2, 5′-UUUGGAACAGAUAU CCAGGGCGACG-3′; and #3, 5′-AAUUCGUGUCCAUUC AGGCUGUAGG-3′), two different negative control siRNAs (#1, Medium GC Duplex; and #2, Low GC Duplex, Life Technologies), or sterile water (vehicle control) were transfected to ZK-1 cells with Lipofectamine RNAiMAX reagents (Life Technologies) by reverse transfection according to the manufacturer's instructions. After 48 h transfection, the cells were trypsinized and plated in fresh media (as day 0). The cells were harvested at days 3 and 5 after re-plating. Effects of RNAi were evaluated by real-time PCR and western blotting.

Immunofluorescence

SCC cells were seeded in chamber slides (Lab-Tek II, Nunc, Thermo Fisher Scientific) and were fixed in 4% paraformaldehyde in PBS for 30 min on ice. Permeabilization was performed by adding 0.2% Triton X-100 to the fixative for 20 min. Cells were incubated with 2% normal goat serum in PBS and then reacted with the primary antibodies overnight at 4 °C. After washing with PBS, cells were further reacted with following secondary antibodies for 1 h at room temperature. For MFG-E8 staining, Alexa Fluor 488-conjugated goat antibodies against mouse IgG (H + L) (Life Technologies) were used as the secondary antibodies. Cells were then counterstained with Hoechst 33258 (Sigma-Aldrich Co., St Louis, MO, USA). For geminin and cleaved caspase-3, the immunoperoxidase method was utilized to obtain their positive ratios, which were determined with mean values calculated by counting positive cells among 400 cells in three different fields.

TdT-Mediated dUTP Nick-End Labeling (TUNEL)

In situ detection of apoptotic cells in formalin-fixed paraffin sections was performed by the TUNEL method using POD In Situ Cell Death Detection Kit (Roche Diagnostics GmbH, Mannheim, Germany) according to the manufacturer's instructions. In brief, tissue sections were pretreated with microwave for 5 min in citrate buffer (pH 6.0). Samples were then reacted with TUNEL reaction mixtures for 1 h at 37 °C and incubated with converter-POD for 30 min at 37 °C. Peroxidase reaction products were developed with 3,3′-diaminobenzidine, and the sections were counterstained with hematoxylin. In the same way, TUNEL signals were demonstrated in cells in culture, though cultured cells were fixed with 4% paraformaldehyde and permeabilized with 0.2% Triton X-100/PBS prior to incubation with the TUNEL reagents. For negative control, sections and cells were incubated with the TUNEL reaction mixtures without TdT. For positive controls, they were treated with DNase I (1 μg/ml) for 10 min at 37 °C. TUNEL+ cell ratios were determined in cultured cells as mentioned above for geminin or cleaved caspase-3.

Western Blotting

Cells cultured in 60-mm dishes were lysed with 150 μl of lysis buffer (50 mM HEPES (pH7.4), 150 mM NaCl, 1% Triton X-100) containing a protease inhibitor cocktail (Nakalai Tesque, Kyoto, Japan). Protein concentrations of cell lysate samples were determined by a standard Bradford assay. An aliquot of 10 μg of proteins was subjected to sodium dodecyl sulfate-polyacrylamide gel electrophoresis (SDS-PAGE) under reducing conditions, and the proteins were transferred to polyvinylidene difluoride membranes (Bio-Rad). After incubation with 0.5% ECL blocking agent (GE Healthcare UK, Little Chalfont, UK) in 50 mM Tris-buffered saline (TBS) (pH 7.4) containing 0.1% Tween-20 (TTBS) for 1 h at room temperature, the membranes were further incubated overnight at 4 °C with primary antibodies diluted with TTBS. Following washing with TTBS, the membranes were reacted with Envision plus (diluted at 1:1000 in TTBS) for 1 h at room temperature. Target protein bands were visualized by ECL Prime western blotting detection reagents (GE Healthcare, UK).

Isolation of Cell Surface Proteins

Proteins expressed on the cell surface were extracted using a Cell Surface Protein Isolation Kit (Pierce, Thermo Fisher Scientific) according to the manufacturer's instructions. Briefly, cultured cells were biotinylated with EZ-Link Sulfo-NHS-SS-biotin for 30 min at 4 °C. After quenching with TBS, cells were lysed with lysis buffer. Cell lysates were applied to spin columns filled with NeutrAvidin gel and incubated for 1 h with end-over-end mixing using a rotator. After the gel was washed, proteins were eluted with SDS-PAGE sample buffer containing 50 mM dithiothreitol. Input, flow-through, and eluted fractions were analyzed by western blotting. Control experiments were performed without biotinylation.

Cell Proliferation Assay

ZK-1 cells were transfected with MFG-E8 siRNA (Msi) or control siRNA (Csi) 48 h prior to following functional assays. Transfected cells were seeded at a density of 3×10^4 in 35-mm dishes. At days 1, 3, and 5 after re-plating, cell numbers were manually counted to make cell growth curves.

Apoptosis Assay

Apoptotic cell rates were evaluated by flow cytometry using a MEBCYTO Apoptosis kit (MBL Co., Ltd., Nagoya, Japan). Cells transfected with siRNA were plated at a concentration of 1.0×10^5 into 60-mm dishes and incubated for 5 days at 37 °C. After incubation, cells were treated and stained with Annexin V-FITC and propidium iodide (PI) according to the distributor's protocols. The treated cells were applied on a BD FACS Aria II Cell Sorter (BD Biosciences, Franklin Lakes, NJ, USA). To determine cell populations in the early or late apoptotic stages, annexin V+/PI-negative (−) ratios or annexin V+/PI+ ratios were calculated, respectively, for the three siRNA-conditioned cells.

Scratch Wound-Healing Assay

An artificial wound was generated on confluent monolayers of vehicle, Csi, and Msi cells in 60-mm culture dishes with a 200-μl yellow pipette tip. Their processes of filling wound areas by migrating cells were monitored under a phase-contrast microscope equipped with a digital camera at 0, 6, 12, 18, and 24 h after plating.

Matrigel Invasion Assay

Cell invasion was determined by using BD Falcon cell culture insert 12-well companion tissue culture plate systems, with an 8-μm pore size polyethylene terephthalate membrane (BD Biosciences). The insert membranes were coated with 50 μl of BD Matrigel (BD Biosciences) diluted at 1:1 with DMEM and then air-dried. Cells at a concentration of 1.0×10^5 were seeded in 1 ml of FCS-free DMEM in the insert chamber, and the lower chamber was filled with 2 ml of DMEM containing 10% FCS. After 24-h incubation, cells in the insert chamber were carefully removed with cotton swabs, and the bottom membrane was fixed with 4% paraformaldehyde and stained with HE. Cells traversing the membrane pores were counted under a microscope, and the mean values were calculated from triplicate experiments.

Statistical Analysis

These statistical analyses were performed using the JMP9 software (SAS Institute Inc., Cary, NC, USA) or GraphPad Prism 4 software (GraphPad Software, Inc., La Jolla, CA, USA). A chi-square test was used to assess the association among categorical data. Differences in continuous variables grouped by patients' histopathological characteristics were evaluated by the Wilcoxon's rank-sum test. Comparative experimental data were analyzed by *t*-test or one-way ANOVA. A P-value < 0.05 was considered statistically significant.

RESULTS

MFG-E8 Immunohistochemistry

MFG-E8 was not detectable in normal squamous epithelia of the oral mucosa (Figure 1a). In the subepithelial connective tissue, MFG-E8 was positive in ductal and acinar cells of mucous glands and endothelial cells of muscular blood vessels (Figure 1b). There was no obvious staining in macrophages. However, in 44 of the 53 cases (83%) of oral SCC, MFG-E8+ carcinoma cells were recognized. Their staining intensities and areas with MFG-E8+ cells varied from case to case (Figures 1c–f). Its strongest staining was obtained in SCC cells forming smaller foci at the invading front (Figure 1c), especially in singularly isolated cells invading muscle tissues (Figure 1g). At higher magnification, MFG-E8 was diffusely localized in the cytoplasm of SCC cells (Figure 1h). In addition, MFG-E8 was intensively localized in apoptotic SCC

Figure 1 Immunohistochemical profiles for milk fat globule—epidermal growth factor—factor VIII (MFG-E8) in normal epithelia and squamous cell carcinoma (SCC) of the oral mucosa. Normal epithelial parts (**a**, **b**) and SCC (**c**–**h**) of the tongue; (**a**–**h**) immunoperoxidase stain for MFG-E8, hematoxylin counter stain. (**a**, **b**, **d**–**f**), ×200; (**c**), ×40; (**g**), ×400, (**h**), ×600. In normal mucosa, there was no positive staining for MFG-E8 in the covering squamous epithelium or in the lamina propriae (**a**). In the submucosal layer, MFG-E8 was localized in ductal and acinar epithelial cells of the mucous gland or in endothelial cells of muscular blood vessels (**b**). In SCC, carcinoma cells showed varying staining patterns from strong (**c**, **d**), to weak (**e**), to nothing (**f**). Intensive staining was observed in SCC cells forming smaller foci (**c**) and in singularly isolated cells (**g**) in the invasive front towards muscle tissues. Within invading SCC foci, MFG-E8 was diffusely positive in the cytoplasm of SCC cells (**h**). In addition, MFG-E8 was concentrated in apoptotic SCC cells, some of which seemed to be engulfed by neighboring living SCC cells (**h**, arrows).

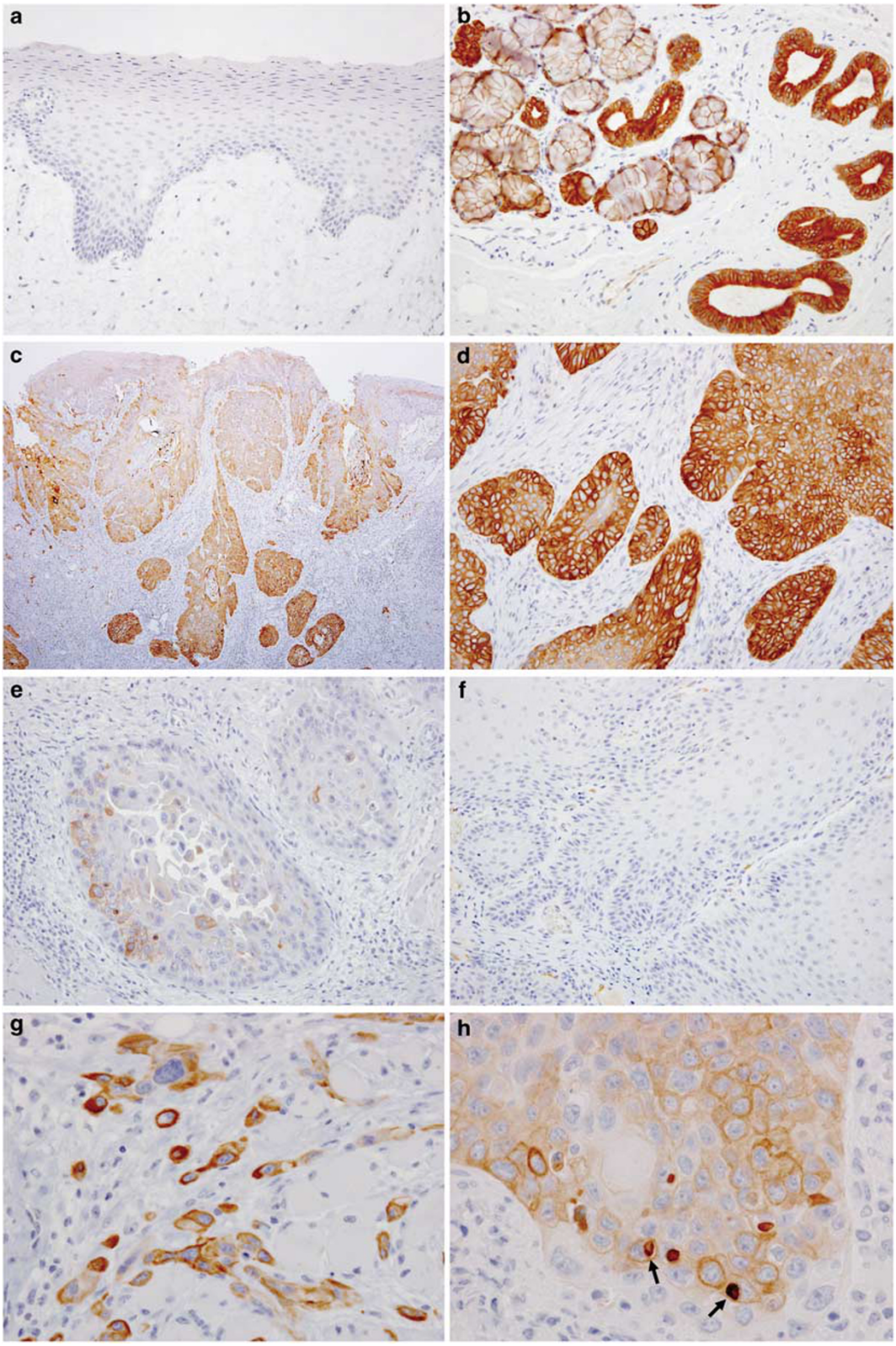

Figure 1 For caption please refer page 1263.

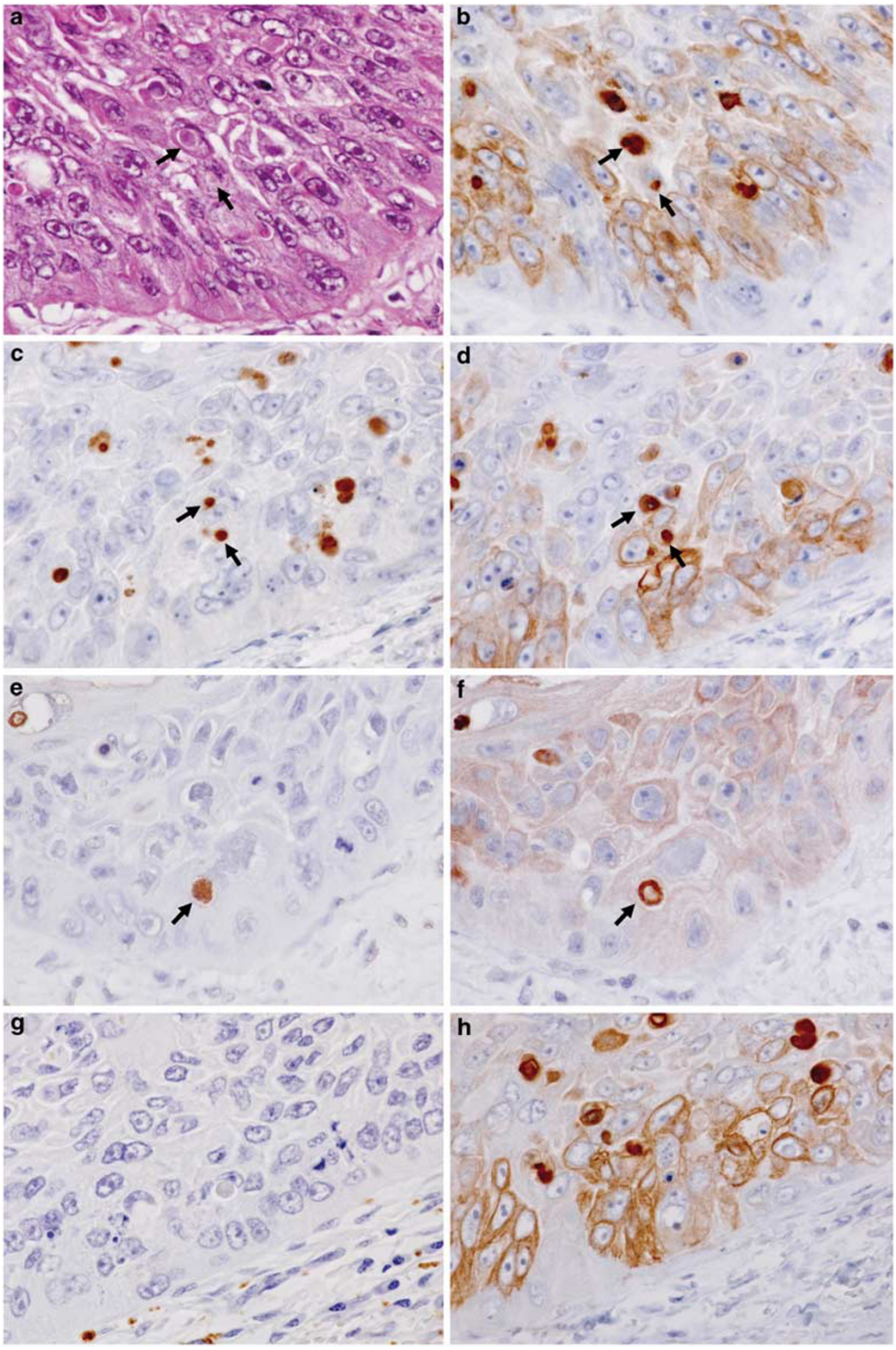

Figure 2 Comparative immunohistochemical profiles between MFG-E8 and related molecules in mirror sections. (**a**) HE stain; immunoperoxidase stain for MFG-E8 (**b**, **d**, **f**, **h**), cleaved caspase-3 (**c**), TdT-mediated dUTP nick-end labeling (TUNEL) staining (**e**), and CD68 (**g**); (**a-b**, **c-d**, **e-f**, **g-h**) four combinations of mirror sections; (**b**, **d**, **f**, **h**) horizontal flips of **a**, **c**, **e**, and **g**, respectively. (**a**–**h**), ×600. Most of the apoptotic SCC cells (**a**) were strongly positive for MFG-E8 (**b**). Some of them were apparently engulfed by neighboring SCC cells, which contained MFG-E8-positive (+) apoptotic bodies in their cytoplasm (**b**, arrows). MFG-E8+ apoptotic bodies or cells (**d**, **f**, arrows) were simultaneously positive for cleaved caspase-3 (**c**, arrows) and TUNEL (**e**, arrows). In the same SCC cell foci, however, CD68+ macrophages were not recognized (**g**, **h**).

cells, some of which were apparently engulfed by neighboring SCC cells (Figure 1h).

In 33 of the 53 SCC cases (62%), we could identify apoptotic SCC cells engulfed by neighboring SCC cells and included in their cytoplasm (Figure 2a, arrows). To demonstrate immunohistochemical profiles in identical SCC cells, we used mirror sectioning (Figures 2a–h), because apoptotic cells were so small that their identical apoptotic bodies could not be visible on serial sections. Most of the apoptotic SCC cells, including engulfed ones, showed strong MFG-E8 positivities (Figures 2a and b). MFG-E8+ apoptotic SCC cells were at the same time positive for cleaved caspase-3 (Figures 2c and d) and TUNEL (Figures 2e and f). There was no obvious infiltration of CD68+ macrophages within MFG-E8+ SCC cell nests (Figures 2g and h).

Clinicopathological Significance of MFG-E8

As a result of MFG-E8 scoring, 9 cases were graded as score 0, 8 as score 1, 8 as score 2, 15 as score 3, and 13 as score 4, with a median of 3. Based on their scores, 53 cases were grouped into two categories: low expression (a score of ≤ 2, 25 cases) and high expression (a score of ≥ 3, 28 cases). Clinicopathological parameters were correlated with the two groups as shown in Table 1. The high MFG-E8 expression group was significantly correlated with advanced pathological stages ($P=0.045$), though it was associated with neither pathological T factors nor lymph node metastases. Both maximal diameters ($P=0.025$) and depth of SCC masses ($P=0.002$) were significantly larger in the high expression group than in the lower expression group (Figures 3a and b). Patients of the high expression group had higher frequencies of locoregional recurrence than did those of the low expression group ($P=0.013$). When patients were separated by age, those ≥ 67 years tended to belong to the high expression group, and their correlation was statistically significant ($P=0.001$). In addition, cases with scattering invasion patterns (singularly isolated SCC cells at invading fronts) were more frequently observed in the high expression group ($P=0.013$). Interestingly, phagocytic figures of SCC cells were more frequently found in the high expression group ($P<0.001$).

Table 1 Relationship between MFG-E8 expression level and clinicopathological factors

		MFG-E8 expression score		
	Case no.	Low (≤ 2)	High (≥ 3)	*P*-value
Age, years				
<67	24	16	8	0.001
≥ 67	29	9	20	
Sex				
Female	24	12	12	0.707
Male	29	13	16	
Pathological T factor				
1	34	18	16	0.260
2–4	19	7	12	
Lymph node metastasis				
Absent	42	22	20	0.138
Present	11	3	8	
Pathological stage				
I–III	40	22	18	0.045
IV	13	3	10	
Locoregional recurrence				
Absent	38	22	16	0.013
Present	15	3	12	
Differentiation				
Well	46	24	22	0.061
Moderate	7	1	6	
Scattering invasion pattern				
Absent	13	10	3	0.013
Present	40	15	25	
Phagocytosis of apoptotic cells by carcinoma cells				
Absent	20	18	2	<0.001
Present	33	7	26	

MFG-E8 Expression in SCC Cells in Culture

We examined MFG-E8 expression modes in three SCC cell lines (ZK-1, ZK-2, and MK-1) and a leukemia cell line (THP-1). MFG-E8 was expressed in those four cell types. In both mRNA (Figure 4a) and protein (Figure 4b) levels, the three types of SCC cells showed higher MFG-E8 expressions than the THP-1 cells did. Among the three SCC cell types, MFG-E8 was most pronounced in ZK-1 (Figures 4a and b), and thus we chose ZK-1 in the following functional experiments. In immunofluorescence, MFG-E8 was confined to the cytoplasm and the outer boundary of ZK-1 cells when they were permeabilized with Triton X-100 (Figure 4c, left panel), while it was in a dot-like pattern only on the outer cell boundary when cells were not permeabilized (Figure 4c, right panel). To determine the subcellular localization of MFG-E8, we separated the cell surface fraction by spin columns and biotinylated cells. Under biotinylation conditions, a band of MFG-E8 at 46 kDa was obviously condensed in the elution fraction but faint in the flow-through fraction (Figure 4d),

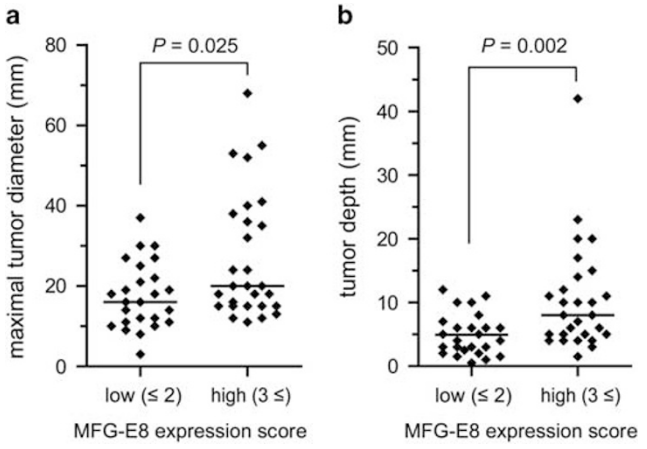

Figure 3 MFG-E8 expression levels and tumor mass sizes represented by diameters (**a**) and depth (**b**). Bars: median. MFG-E8 expression profiles were scored by positive staining areas and their intensities of SCC in 53 cases in the manner described in the Materials and Methods section. The cases were further divided into two groups according to their MFG-E8 scores: a low expression group (a score of ≤ 2) and a high expression group (a score of ≥ 3). Both maximum diameters (**a**, $P = 0.025$) and depth (**b**, $P = 0.002$) of the tumor masses were significantly larger in SCC cases of the high expression group than in those of the low expression group (Wilcoxon's rank-sum test).

whereas the band was mainly found in the flow-through fractions when cells were not biotinylated. These results indicated that MFG-E8 was localized on the cell surface in addition to within the cytoplasm. The finding also confirmed by immunofluorescence staining performed with and without permeabilization suggested that some of the synthesized MFG-E8 molecules were secreted onto the cell surface.

MFG-E8 Functions in SCC Cells

To examine the function of MFG-E8, we attempted a temporary knockdown of MFG-E8 by using siRNA in ZK-1 cells, which expressed the highest amounts of MFG-E8, as mentioned above. Up to day 5 after plating, MFG-E8 gene expression levels were significantly suppressed by the three siRNA sequences (Msi cells) when compared with those in controls (vehicle and Csi cells) (Figure 5a). However, MFG-E8 protein levels were not effectively diminished at 48 h after siRNA transfection (data not shown). Even at day 5 after plating, MFG-E8 protein bands were not completely abolished in Msi cells, though they were obviously reduced (Figure 5b). The most effective siRNA sequence was Msi #2, followed by Msi #1. However, Msi #3 did not work as

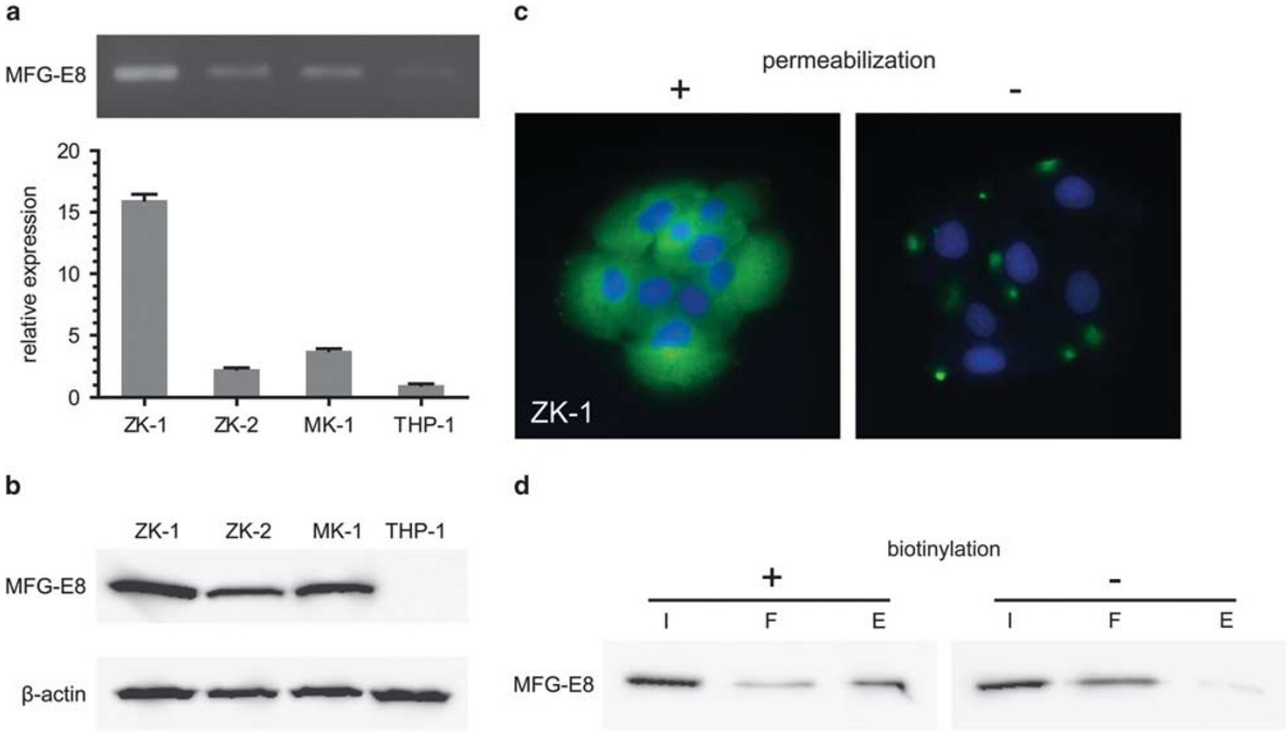

Figure 4 MFG-E8 expression profiles in oral SCC cell lines. (**a**) mRNA expression levels by reverse transcription PCR (RT-PCR); protein expression levels by western blotting (**b**), immunofluorescence (**c**, green, MFG-E8; blue, Hoechst 33258), and western blotting for cell surface proteins (**d;** I, input; F, flow-through; E, eluted fractions). MFG-E8 expressions at gene (**a**) and protein (**b**) levels were confirmed in three oral SCC cell lines, ZK-1, ZK-2 and MK-1. Among them, ZK-1 showed the most enhanced levels, while THP-1 of leukemia origin scarcely expressed MFG-E8. In ZK-1, MFG-E8 immunofluorescence signals were diffusely localized in the cytoplasm after permeabilization (**c**, +/left), though they were demonstrated in large dot-like patterns on the cell surface or boundary before permeabilization (**c**, −/right). After cell surface proteins of ZK-1 were biotinylated (**d**, +/left), cell lysates (I) were separated with avidin-conjugated columns into flow-through (F) and eluted (E) fractions. Western blotting demonstrated that MFG-E8 was found in both the flow-through (cytoplasm) and eluted (the cell surface) fractions. In control experiments without biotinylation, there was no obvious band in the eluted fractions (**d**, −/right).

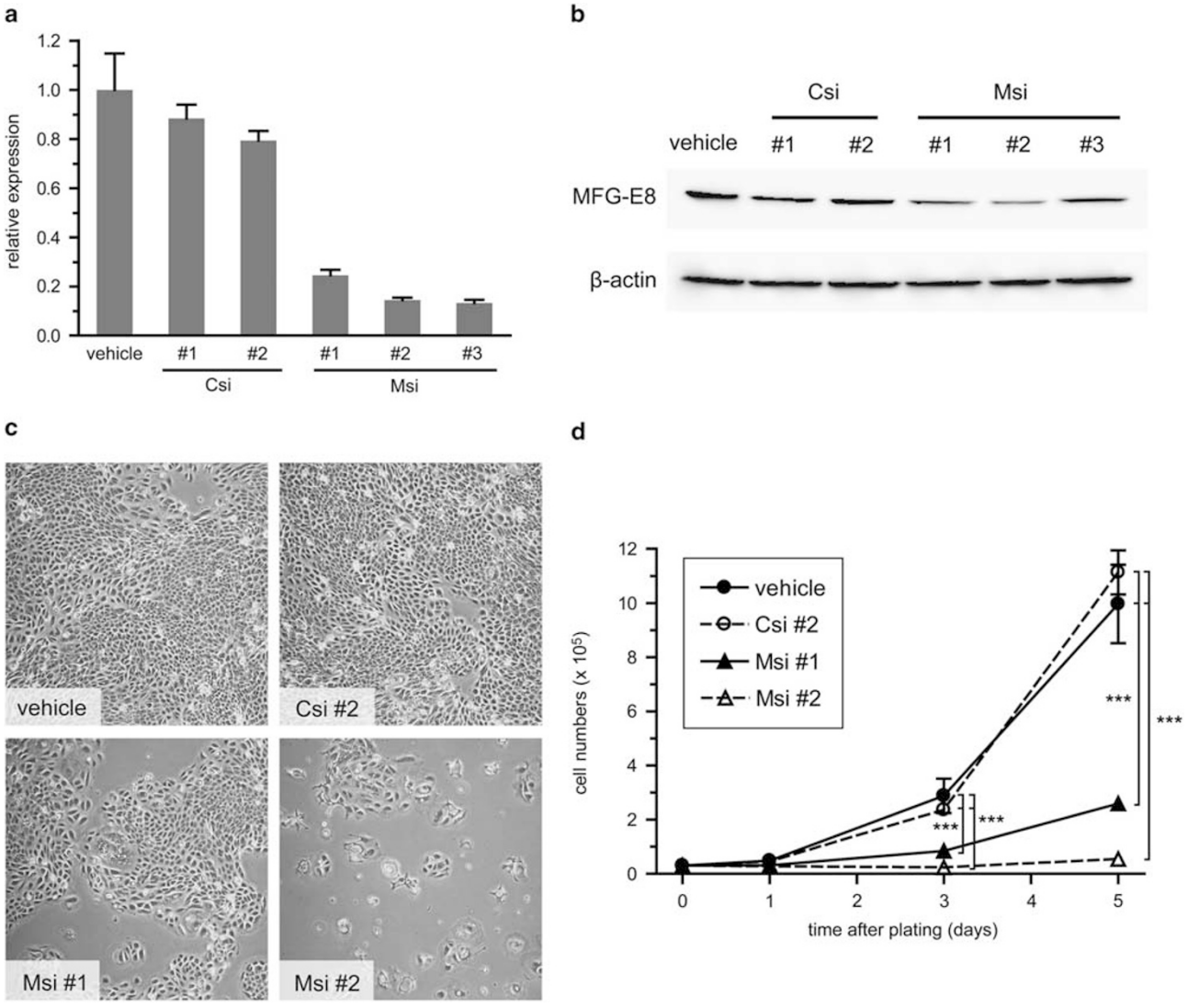

Figure 5 Suppression of MFG-E8 gene expression by RNA interference (RNAi) in ZK-1 cells. (**a**) mRNA expression levels by reverse transcription PCR (RT-PCR); (**b**) protein levels by western blotting: left, vehicle control cells: middle, control siRNA-treated (Csi #1, #2) cells: right, MFG-E8 siRNA-treated (Msi #1-#3) cells; (**c**) phase-contrast images of ZK-1 cells in the four different conditions at day 5 after plating; (**d**) growth curves of ZK-1 cells: closed circles, vehicle: open circles, Csi #2: closed triangles, Msi #1: open triangles, Msi #2. (**a**, **d**) Means ± s.d. (bars) from triplicate experiments. MFG-E8 gene expression levels were effectively suppressed in Msi cells, which were transfected with three different MFG-E8 siRNA sequences (#1–#3), when compared with control cells without vehicle or Csi cells with two different control siRNA sequences (#1 and #2) (**a**). MFG-E8 protein expression levels were reduced to some extent but were not completely suppressed (**b**). Msi cells, especially Msi #2, were apparently smaller in number than vehicle and Csi cells (**c**). Cell growths of Msi cells, especially Msi #2, were significantly inhibited after days 3–5 (***$P<0.001$) (**d**).

effectively as Csi #1 and Csi #2 did. In the following experiment, we used Msi #2, Msi #1, and Csi #2 sequences. We then analyzed the effect of MFG-E8 knockdown on cell growth. Cell numbers of Msi cells, especially of Msi #2 cells, were obviously smaller at day 5, when vehicle and Csi #2 cells reached their confluencies (Figure 5c). When cell numbers were plotted as growth curves, the suppression in proliferation was confirmed in Msi cells at days 3–5 ($P<0.001$) (Figure 5d).

In the following functional experiments for cell proliferation, apoptosis, and invasion, we adopted Msi #2 as the most effective MFG-E8-targeting siRNA and Csi #2 as the negative control siRNA. To evaluate proportions of cells in cell cycles, we performed immunohistochemistry for geminin, which specifically demonstrated cells in the S and early M phases.[24] Geminin-labeling indices in Msi cells were significantly lower than those in vehicle or Csi cells (Figure 6a). The results suggested that MFG-E8 has a role in cell proliferation.

Next, we performed immunohistochemistry for cleaved caspase-3 and TUNEL staining to examine whether suppressed MFG-E8 induced apoptotic cell death (Figures 6b and c). As a result, positive ratios for the two markers were

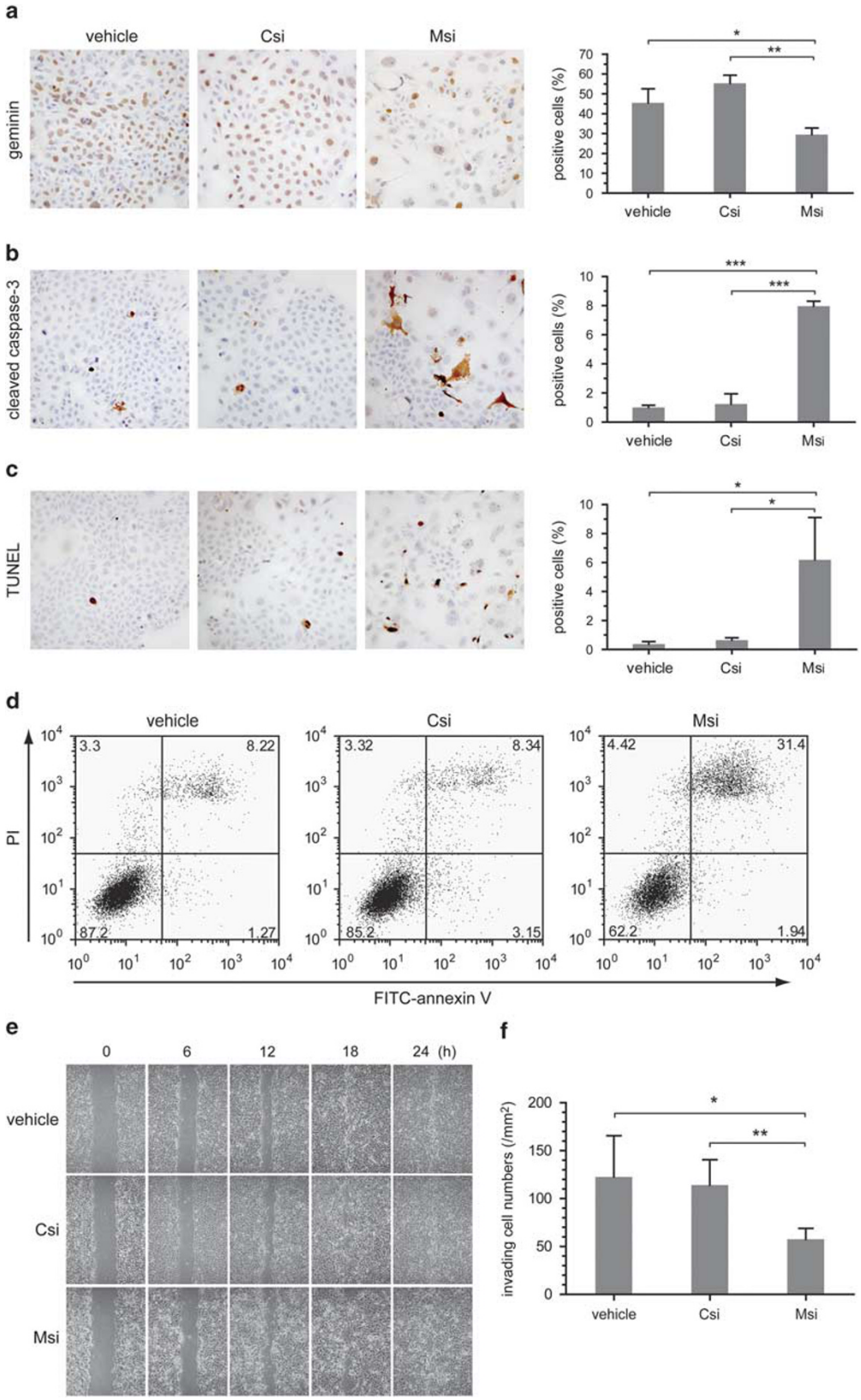

Figure 6 For caption please refer page 1270.

significantly higher in Msi cells than those in vehicle and Csi cells. In flow-cytometric apoptosis assays, annexin V+/PI+ ratios significantly increased in Msi cells (31.4%), indicating that they were in the late apoptotic stages, while early apoptotic cells represented by annexin V+/PI− were not varied in the three conditions (Figure 6d). These results indicate that MFG-E8 functioned to protect against promotion of SCC cell apoptosis.

To examine the MFG-E8 function in cell migration and invasion, we performed scratch wound-healing assays and Matrigel invasion assays, respectively. In scratch wound-healing assays, there was no obvious difference between vehicle, Csi, and Msi cells during the experimental period up to 24 h (Figure 6e). In contrast, the numbers of Msi cells penetrating through Matrigel-coated membranes were significantly decreased at 24 h by approximately 50% compared with vehicle and Csi cells (Figure 6f). Thus, ZK-1 cell invasiveness was shown to be dependent on MFG-E8 expression levels, whereas it did not affect cellular migration activities.

DISCUSSION

In the present study, we have demonstrated for the first time that MFG-E8 is expressed in oral SCC cells and is involved in the phagocytosis of apoptotic SCC cells and that its expression is positively related to SCC cell proliferation, invasion, and viability. Prior to our study, the expression profiles and the functional significance of MFG-E8 had not been explored in human SCCs of any other organs in detail.

We confirmed increased expression of MFG-E8 in oral SCC compared with that of normal oral epithelia by immunohistochemistry. Our immunohistochemical observations in oral SCC tissue specimens were similar to those for other cancer types, such as malignant melanoma,[18,19] urothelial carcinoma of the bladder,[20] and breast adenocarcinoma.[16,17] In addition, we confirmed MFG-E8 expression levels in endothelial cells of muscular blood vessels and salivary gland cells but not in the other cell types, including macrophages or dendritic cells. This was not consistent with previous *in vitro* data from mice, in which thioglycollate-elicited peritoneal macrophages[3] and bone marrow-derived immature dendritic cells[25] express MFG-E8. This discrepancy may be due to much lower expression levels in macrophages, as we demonstrated in cell culture experiments where SCC cells expressed higher levels of MFG-E8 than did THP-1 cells of monocyte/macrophage origin. The results that MFG-E8+ cells tended to be located in singular forms and in invading fronts and that high expression levels of MFG-E8 were correlated with clinicopathological properties like tumor size, pathological stage, locoregional recurrence, and scattering invasion pattern indicate that MFG-E8 can be an indicator of SCC progression. It was shown to be a prognostic factor in malignant melanoma,[19] though we could not analyze its relation to clinical outcome in the present series of patients due to ethical approval procedures.

Apoptotic cancer cells are believed to be cleared by macrophages. Also, phagocytosis of dead or living cancer cells by cancer cells themselves (cannibalism) has been known to pathologists for long time,[26] although no particular attention has been paid to whether or not cancer cell deaths are due to apoptosis. Rather than engulfing apoptotic cancer cells,[27–29] cancer cells are also able to phagocytose neutrophils,[30] lymphocytes,[31] and erythrocytes.[32,33] This has been was widely recognized in diagnostic cytology, in which these cell-engulfing features have practically been used as the definitive evidence of malignancy.[34] However, the molecular mechanisms underlying this phenomenon still remain entirely unknown. Recently, D'Mello *et al*[28] reported that urokinase plasminogen activator receptor promotes apoptotic cell clearance by cancer cells by using a mechanism independent from $\alpha v\beta 5$-mediated clearance. As we showed in the present study, apoptotic SCC cells were strongly positive for MFG-E8, and they were simultaneously shown within the cytoplasm of neighboring SCC cells. Moreover, we were successful in demonstrating cell surface MFG-E8 in oral SCC cells in culture in addition to within the cytoplasm, suggesting that MFG-E8 is secreted to the cell surface. These findings indicate that MFG-E8 secreted by SCC cells binds to apoptotic SCC cells to be engulfed easily by neighboring cells, which is similar to MFG-E8-dependent eat-me signals observed in the mammary gland involution.[14]

The MFG-E8 overexpression has been correlated to tumor progression via multiple pathways in several types of cancer cells.[17,18,35] Jinushi *et al* demonstrated that MFG-E8 raises resistance to apoptosis via an Akt-dependent pathway and trigger an epithelial-to-mesenchymal transition (EMT) through Twist-dependent pathways, resulting in increased invasiveness and metastatic capacity in mouse melanoma models.[18] MFG-E8 also coordinates cell cycle molecules such

Figure 6 MFG-E8 functional assays for proliferation, apoptosis, migration, and invasion by RNAi in ZK-1. (**a**) left: immunoperoxidase stain for geminin, right: geminin-labeling indices at day 5; (**b**) left: immunoperoxidase stain for cleaved caspase-3, right: cleaved caspase-3-positive (+) cell ratios at day 5; (**c**) left: TUNEL staining, right: TUNEL+ cell ratios at day 5; (**d**) flow cytometric analysis for apoptosis by dual staining with annexin V *vs* propidium iodide (PI) at day 5; (**e**) scratch wound-healing assays for 24 h; (**f**) Invasion assays of ZK-1 cells in Matrigel at 24 h, cell counts per mm^2. (**a**–**c**, **f**) Means ± s.d. from triplicate experiments. $^*P<0.05$, $^{**}P<0.01$, $^{***}P<0.001$. When proportions of cells in cell cycle phases were demonstrated by geminin-labeling indices, the indices of Msi #2 cells were significantly lower than those of vehicle and Csi (#2) cells (**a**), whereas ratios of cleaved caspase-3+ cells (**b**) and TUNEL+ cells (**c**) in Msi (#2) cells were instead significantly higher than those of vehicle and Csi cells. Ratios of annexin V+/PI+ cells were significantly higher in Msi cells than those in vehicle and Csi cells (**d**). There was no definite difference in cell migration among the three conditions (**e**). In contrast, Msi cells invading through Matrigel-coated membranes were significantly smaller in number than vehicle and Csi cells (**f**).

as proliferating cell nuclear antigen and cyclin-dependent kinase 4 to facilitate cell proliferation via integrin/ERK1/2 signaling in vascular smooth muscle cells.[36] Our present MFG-E8 knockdown experiment clearly indicated that MFG-E8 facilitates cell proliferation and acts as an anti-apoptotic factor in oral SCC. When MFG-E8 was suppressed in the present study, geminin+ cells, which were about to divide, decreased in number, while apoptotic cells, which were revealed by activation of caspase-3 and DNA fragmentation, increased in number. The geminin reduction in MFG-E8-suppressed cells is thus considered reasonable, because geminin is one of the molecules that are degraded by cleaved caspase-3.[37] The repressed invasion of MFG-E8-suppressed cells is consistent with the results reported by Jinushi *et al*,[18] in which EMT was accelerated in MFG-E8-overexpressing melanoma cells. Similar mechanisms might be underlying in oral SCC cells, too. We speculate engulfment of apoptotic cells itself also activates cell proliferation and survival. In addition to those direct effects on cancer cells, MFG-E8 must be involved in some immune system-dependent mechanism including tolerogenic T lymphocyte induction, which promotes cancer cells to grow.[20,35]

In conclusion, we have demonstrated that MFG-E8 promotes tumor progression in oral SCC and that it is involved in the clearance of apoptotic SCC cells by neighbor SCC cells. Further investigation is needed to determine whether MFG-E8 promotes apoptotic cell engulfment by cancer cells and to clarify its functions in various aspects of cancer cell activities, possibly leading to anti-cancer therapeutic strategies.

ACKNOWLEDGMENTS

This study was supported by Grants-in-Aid for Scientific Research from the Japan Society for Promotion of Science (JSPS) (to MY, SM, TA, JC, and TS).

DISCLOSURE/CONFLICT OF INTEREST

The authors declare no conflict of interest.

1. Ceriani RL, Sasaki M, Sussman H, *et al.* Circulating human mammary epithelial antigens in breast cancer. Proc Natl Acad Sci USA 1982; 79:5420–5424.
2. Stubbs JD, Lekutis C, Singer KL, *et al.* cDNA cloning of a mouse mammary epithelial cell surface protein reveals the existence of epidermal growth factor-like domains linked to factor VIII-like sequences. Proc Natl Acad Sci USA 1990;87:8417–8421.
3. Hanayama R, Tanaka M, Miwa K, *et al.* Identification of a factor that links apoptotic cells to phagocytes. Nature 2002;417:182–187.
4. Ensslin MA, Lyng R, Raymond A, *et al.* Novel gamete receptors that facilitate sperm adhesion to the egg coat. Soc Reprod Fertil Suppl 2007;63:367–383.
5. Raymond AS, Shur BD. A novel role for SED1 (MFG-E8) in maintaining the integrity of the epididymal epithelium. J Cell Sci 2009;122: 849–858.
6. Bu HF, Zuo XL, Wang X, *et al.* Milk fat globule-EGF factor 8/lactadherin plays a crucial role in maintenance and repair of murine intestinal epithelium. J Clin Invest 2007;117:3673–3683.
7. Ensslin MA, Shur BD. The EGF repeat and discoidin domain protein, SED1/MFG-E8, is required for mammary gland branching morphogenesis. Proc Natl Acad Sci USA 2007;104:2715–2720.
8. Silvestre JS, Thery C, Hamard G, *et al.* Lactadherin promotes VEGF-dependent neovascularization. Nat Med 2005;11:499–506.
9. Larocca D, Peterson JA, Urrea R, *et al.* A Mr 46,000 human milk fat globule protein that is highly expressed in human breast tumors contains factor VIII-like domains. Cancer Res 1991;51:4994–4998.
10. Couto JR, Taylor MR, Godwin SG, *et al.* Cloning and sequence analysis of human breast epithelial antigen BA46 reveals an RGD cell adhesion sequence presented on an epidermal growth factor-like domain. DNA Cell Biol 1996;15:281–286.
11. Ensslin M, Vogel T, Calvete JJ, *et al.* Molecular cloning and characterization of P47, a novel boar sperm-associated zona pellucida-binding protein homologous to a family of mammalian secretory proteins. Biol Reprod 1998;58:1057–1064.
12. Hanayama R, Tanaka M, Miyasaka K, *et al.* Autoimmune disease and impaired uptake of apoptotic cells in MFG-E8-deficient mice. Science 2004;304:1147–1150.
13. Jinushi M, Nakazaki Y, Dougan M, *et al.* MFG-E8-mediated uptake of apoptotic cells by APCs links the pro- and antiinflammatory activities of GM-CSF. J Clin Invest 2007;117:1902–1913.
14. Hanayama R, Nagata S. Impaired involution of mammary glands in the absence of milk fat globule EGF factor 8. Proc Natl Acad Sci USA 2005;102:16886–16891.
15. Fens MH, Mastrobattista E, de Graaff AM, *et al.* Angiogenic endothelium shows lactadherin-dependent phagocytosis of aged erythrocytes and apoptotic cells. Blood 2008;111:4542–4550.
16. Yang C, Hayashida T, Forster N, *et al.* The integrin alpha(v)beta(3-5) ligand MFG-E8 is a p63/p73 target gene in triple-negative breast cancers but exhibits suppressive functions in ER(+) and erbB2(+) breast cancers. Cancer Res 2011;71:937–945.
17. Carrascosa C, Obula RG, Missiaglia E, *et al.* MFG-E8/lactadherin regulates cyclins D1/D3 expression and enhances the tumorigenic potential of mammary epithelial cells. Oncogene 2012;31:1521–1532.
18. Jinushi M, Nakazaki Y, Carrasco DR, *et al.* Milk fat globule EGF-8 promotes melanoma progression through coordinated Akt and twist signaling in the tumor microenvironment. Cancer Res 2008;68: 8889–8898.
19. Oba J, Moroi Y, Nakahara T, *et al.* Expression of milk fat globule epidermal growth factor-VIII may be an indicator of poor prognosis in malignant melanoma. Br J Dermatol 2011;165:506–512.
20. Sugano G, Bernard-Pierrot I, Lae M, *et al.* Milk fat globule-epidermal growth factor-factor VIII (MFGE8)/lactadherin promotes bladder tumor development. Oncogene 2011;30:642–653.
21. Tibaldi L, Leyman S, Nicolas A, *et al.* New blocking antibodies impede adhesion, migration and survival of ovarian cancer cells, highlighting MFGE8 as a potential therapeutic target of human ovarian carcinoma. PLoS One 2013;8:e72708.
22. Watanabe T, Totsuka R, Miyatani S, *et al.* Production of the long and short forms of MFG-E8 by epidermal keratinocytes. Cell Tissue Res 2005;321:185–193.
23. Osamura RY, Watanabe K, Nakai Y, *et al.* Adrenocorticotropic hormone cells and immunoreactive beta-endorphin cells in the human pituitary gland: normal and pathologic conditions studied by the peroxidase-labeled antibody method. Am J Pathol 1980;99:105–124.
24. McGarry TJ, Kirschner MW. Geminin, an inhibitor of DNA replication, is degraded during mitosis. Cell 1998;93:1043–1053.
25. Miyasaka K, Hanayama R, Tanaka M, *et al.* Expression of milk fat globule epidermal growth factor 8 in immature dendritic cells for engulfment of apoptotic cells. Eur J Immunol 2004;34:1414–1422.
26. Fais S. Cannibalism: a way to feed on metastatic tumors. Cancer Lett 2007;258:155–164.
27. Simamura E, Hirai KI, Shimada H, *et al.* Apoptosis and epithelial phagocytosis in mitomycin C-treated human pulmonary adenocarcinoma A549 cells. Tissue Cell 2001;33:161–168.
28. D'Mello V, Singh S, Wu Y, *et al.* The urokinase plasminogen activator receptor promotes efferocytosis of apoptotic cells. J Biol Chem 2009;284:17030–17038.
29. Lugini L, Lozupone F, Matarrese P, *et al.* Potent phagocytic activity discriminates metastatic and primary human malignant melanomas: a key role of ezrin. Lab Invest 2003;83:1555–1567.
30. Caruso RA, Muda AO, Bersiga A, *et al.* Morphological evidence of neutrophil-tumor cell phagocytosis (cannibalism) in human gastric adenocarcinomas. Ultrastruct Pathol 2002;26:315–321.
31. Lugini L, Matarrese P, Tinari A, *et al.* Cannibalism of live lymphocytes by human metastatic but not primary melanoma cells. Cancer Res 2006;66:3629–3638.

32. Monteagudo C, Jorda E, Carda C, *et al*. Erythrophagocytic tumour cells in melanoma and squamous cell carcinoma of the skin. Histopathology 1997;31:367–373.
33. Al-Eryani K, Cheng J, Abé T, *et al*. Hemophagocytosis-mediated keratinization in oral carcinoma in situ and squamous cell carcinoma: a possible histopathogenesis of keratin pearls. J Cell Physiol 2013;228: 1977–1988.
34. Kojima S, Sekine H, Fukui I, *et al*. Clinical significance of "cannibalism" in urinary cytology of bladder cancer. Acta Cytol 1998;42:1365–1369.
35. Jinushi M, Sato M, Kanamoto A, *et al*. Milk fat globule epidermal growth factor-8 blockade triggers tumor destruction through coordinated cell-autonomous and immune-mediated mechanisms. J Exp Med 2009;206:1317–1326.
36. Wang M, Fu Z, Wu J, *et al*. MFG-E8 activates proliferation of vascular smooth muscle cells via integrin signaling. Aging Cell 2012;11:500–508.
37. Roukos V, Iliou MS, Nishitani H, *et al*. Geminin cleavage during apoptosis by caspase-3 alters its binding ability to the SWI/SNF subunit Brahma. J Biol Chem 2007;282:9346–9357.